Science Advances

AAAS

advances.sciencemag.org/cgi/content/full/3/7/e1603208/DC1

Supplementary Materials for

Reconstitution of calcium-mediated exocytosis of dense-core vesicles

Alex J. B. Kreutzberger, Volker Kiessling, Binyong Liang, Patrick Seelheim, Shrutee Jakhanwal, Reinhard Jahn, J. David Castle, Lukas K. Tamm

Published 19 July 2017, *Sci. Adv.* **3**, e1603208 (2017)
DOI: 10.1126/sciadv.1603208

This PDF file includes:

(lipid/protein = 3000) incubated with 2 μM synaptobevin-2 (residues 1 to 96) inhibitor peptide.

- table S2. Event statistics for DCV docking and fusion to planar supported bilayers with syntaxin-1a (residues 183 to 288):SNAP-25 (lipid/protein = 3000) with increasing concentration of divalent metals (Ca^{2+} and Mg^{2+}).
- table S3. Fit values of a parallel reaction model [$N(t) = N(1 - e^{-kt})^m$, where N is the fusion probability, k is the rate, and m is the number of parallel reactions occurring] for the cumulative distribution function of delay times between docking and fusion for single-particle DCV events with different concentrations of divalent metals.
- table S4. Fits of ensemble lipid mixing data shown in fig. S3.
- table S5. Event statistics for docking and fusion of DCVs to planar supported bilayers with 5% $PI(4,5)P_2$ [bPC:bPE:bPS:Chol:$PI(4,5)P_2$ (25:25:15:30:5)], 3% $PI(4,5)P_2$ [bPC:bPE:bPS:Chol:PI:$PI(4,5)P_2$ (25:25:15:30:2:3)], 1% $PI(4,5)P_2$ [bPC:bPE:bPS:Chol:PI:$PI(4,5)P_2$ (25:25:15:30:4:1)], 0% $PI(4,5)P_2$ [bPC:bPE:bPS:Chol:PI (25:25:15:30:5)], and no charged lipids [bPC:bPE:Chol (35:35:30)] in the presence of 100 μM EDTA or 100 μM Ca^{2+}.
- table S6. Event statistics for docking and fusion of DCVs to planar supported bilayers with 5% $PI(4,5)P_2$ [bPC:bPE:bPS:Chol:$PI(4,5)P_2$ (25:25:15:30:5)], 3% $PI(4,5)P_2$ [bPC:bPE:bPS:Chol:PI:$PI(4,5)P_2$ (25:25:15:30:2:3)], 1% $PI(4,5)P_2$ [bPC:bPE:bPS:Chol:PI:$PI(4,5)P_2$ (25:25:15:30:4:1)], 0% $PI(4,5)P_2$ [bPC:bPE:bPS:Chol:PI (25:25:15:30:5)], and no charged lipids [bPC:bPE:Chol (35:35:30)] in the presence of 100 μM EDTA or 100 μM Ca^{2+}.
- table S7. Event statistics for DCV docking and fusion to planar supported bilayers with syntaxin-1a (residues 183 to 288):SNAP-25 (lipid/protein = 3000) with wild-type DCVs, DCVs inhibited with antibodies for either syt or CAPS, or DCVs that have had syt or CAPS knocked down using shRNA before purification.
- table S8. Fit values of a parallel reaction model [$N(t) = N(1 - e^{-kt})^m$, where N is the fusion probability, k is the rate, and m is the number of parallel reactions occurring] for the cumulative distribution function of delay times between docking and fusion for single-particle DCV events for conditions described in Fig. 2.
- table S9. Event statistics for DCV docking and fusion to planar supported bilayers containing either syntaxin-1a (residues 183 to 288) or syntaxin-1a (residues 1 to 288) with SNAP-25 (lipid/protein = 3000), with the addition of complexin-1 and/or Munc18 in the presence of 100 μM EDTA or 100 μM Ca^{2+}.
- table S10. Fit values of a parallel reaction model [$N(t) = N(1 - e^{-kt})^m$, where N is the fusion probability, k is the rate, and m is the number of parallel reactions occurring] for the cumulative distribution function of delay times between docking and fusion for single-particle DCV events for conditions described in Fig. 3.
- table S11. Event statistics of triggered fusion of DCVs at different calcium concentrations from data shown in Fig. 4B.
- table S12. Event statistics of spontaneous fusion of DCVs docked in triggering conditions with planar supported bilayers of different lipid compositions.

- table S13. Event statistics of triggered fusion of DCVs with planar supported bilayers of different lipid compositions.
- table S14. Event statistics of spontaneous fusion of DCVs docked in triggering conditions with knockdowns of syt-1/9 or CAPS with subsequent recoveries.
- table S15. Event statistics of triggered fusion of DCVs with knockdowns of syt-1/9 or CAPS and subsequent recoveries.
- table S16. Table of primers described in the "Plasmids and shRNA constructs" section of Materials and Methods.
- table S17. Event statistics for DCV docking and fusion to planar supported bilayers with the indicated combination of proteins syntaxin-1a (residues 183 to 288), syntaxin-1a (residues 1 to 288), and SNAP-25 (lipid/protein = 3000) incubated, as indicated, with Munc18 (0.5 μM), complexin-1 (2 μM), and synaptobrevin-2 (residues 1 to 96) inhibitor peptide.
- table S18. Event statistics for DCV docking and fusion to planar supported bilayers containing syntaxin-1a (residues 1 to 288):SNAP-25, 0.5 μM Munc18, and indicated amounts of complexin-1.
- References (*70–74*)

Supplementary Text

2-step Mathematical Fusion/Diffusion Model to Simulate the Single DCV Fluorescence Intensity Trace

The fluorescence signal originating from the DCVs during spontaneous, Ca^{2+} accelerated, and Ca^{2+} triggered fusion follows a characteristic line shape (Fig. 1C and fig. S1). In the following paragraphs we describe a simple 2-step fusion/diffusion model that reproduces the basic features of the signal.
At each time the fluorescence originating from the fluorophore mRuby is determined by the sum of the fluorophore fraction located in the lumen of the DCV at a concentration C_{DCV} and the fraction in the small cleft between supported membrane and substrate at concentration C_{CLEFT}

$$I = I_{DCV}(C_{DCV}(t,x,y),\lambda) + I_{CLEFT}(C_{CLEFT}(t,x,y,D),\lambda) \quad (1)$$

The model starts with a DCV of diameter d_{DCV} = 200 nm (*66*) docked at the supported lipid bilayer at distance z_0=8 nm (*67*) from the substrate and at x,y = 0. For the observed intensities we take into account the 2D point spread function at λ = 600 nm and the decay of the evanescent wave with a characteristic penetration depth of d_p = 100 nm

$$I_0 = I_{DCV}(t < t_1) = PSF(\lambda) * \int_{z_0}^{z_0+d_{DCV}} C_{DCV}(x,y,z)\, e^{\frac{-z}{d_p}}\, dz \quad (2)$$

At time t_1 a fusion pore opens and content from the DCV gets released through the supported membrane into the cleft with a characteristic rate k_r at x,y = 0

$$r(t - t_1) = e^{-\frac{(t-t_1)}{k_r}} \quad (3)$$

Fluorescent content in the cleft is located at an average distance z_{CLEFT} = 2 nm (*70*) and spreads laterally in the x,y plane by free diffusion characterized by a diffusion coefficient D_1

$$dC_{CLEFT}(t_1 < t < t_2) = [dr + D_1 \Delta C_{CLEFT}]dt \quad (4)$$

$$I_{CLEFT}(t_1 < t < t_2) = PSF(\lambda) * C_{CLEFT}(x, y, z, t)\, e^{\frac{-z_{CLEFT}}{d_p}} \quad (5)$$

During the life time of the fusion pore ($t_1 < t < t_2$) the shape of the DCV stays intact and content gets released from membrane proximal areas first (fig. S1C). A simpler model in which the distribution of content inside the DCV stays homogenous did not fit the data sufficiently. The fluorescence intensity originating from the DCV during this phase becomes

$$I_{DCV}(t_1 < t < t_2) = PSF(\lambda) * \int_{z_1(t)}^{z_0+d_{DCV}} C_{DCV}(x, y, z)\, e^{\frac{-z}{d_p}}\, dz \quad (6)$$

with $z_1(t)$ changing over time as more and more content gets released.

At time t_2 the DCV with its remaining content in the distal region from the supported membrane collapses into the SLB and diffuses together with the already released content laterally within the cleft with a diffusion coefficient D_2

$$C_{CLEFT}(t = t_2) = C_{CLEFT}(x, y, z, t_2) + C_{DCV}(x, y, z, t_2) \quad (7)$$

$$dC_{CLEFT}(t > t_2) = D_2 \Delta C_{CLEFT} dt \quad (8)$$

At the time of collapse (t_2) we assume the remaining content to collapse into a plane corresponding to the surface area of the original DCV instantaneously. The total observable intensity which now originates only from the cleft becomes

$$I_{CLEFT}(t > t_2) = PSF(\lambda) * C_{CLEFT}(x, y, z, t)\, e^{\frac{-z_{CLEFT}}{d_p}} \quad (9)$$

We simulated the fluorescence intensity of the central pixel centered at a DCV using the above parameters and adjusting the length of the time period t_2-t_1, the release rate k_r and the diffusion coefficients $D_{1/2}$. In the shown simulation (fig. S1), the DCVs release fluorescent content at a characteristic rate of 0.7 s^{-1} for the duration of 700 ms. The content diffuses with a rate of D_1 = 5 $\mu m^2/s$; DCVs then collapse into the supported membrane after which the remaining content diffuses with a specific diffusion coefficient of D_2 =0.05 $\mu m^2/s$. This sequence was then used to compute traces for TIRF microscopy (d_p = 100 nm) in (fig. S1A) and epi-fluorescence microscopy (d_p = inf) in (fig.

S1B). Despite the simplifications in the model the curves reproduce the basic characteristics of the recorded traces very well. Both diffusion coefficients are significantly smaller than the reported diffusion coefficient for GFP in solution ($D \approx 80\ \mu m^2/s$, (*71*) indicating that the content indeed diffuses in the cleft between SLB and substrate where the molecular mobility is known to be impaired (*72*, *73*). The slower diffusion observed after the collapse of the DCV might be due to the high density of (protein-) material at the fusion site. The epi-fluorescence recording in (fig. S1B) shows that the characteristic peak observed in the TIRF recording (fig. S1A) is indeed caused by the movement of fluorescent content closer to the surface within the evanescent field. As mentioned above, it was necessary to preserve the overall structure and shape of the DCV during the release phase to model the data sufficiently. This observation agrees well with the explanation for the amperometric foot signals during exocytotic events in chromaffin cells (*74*).

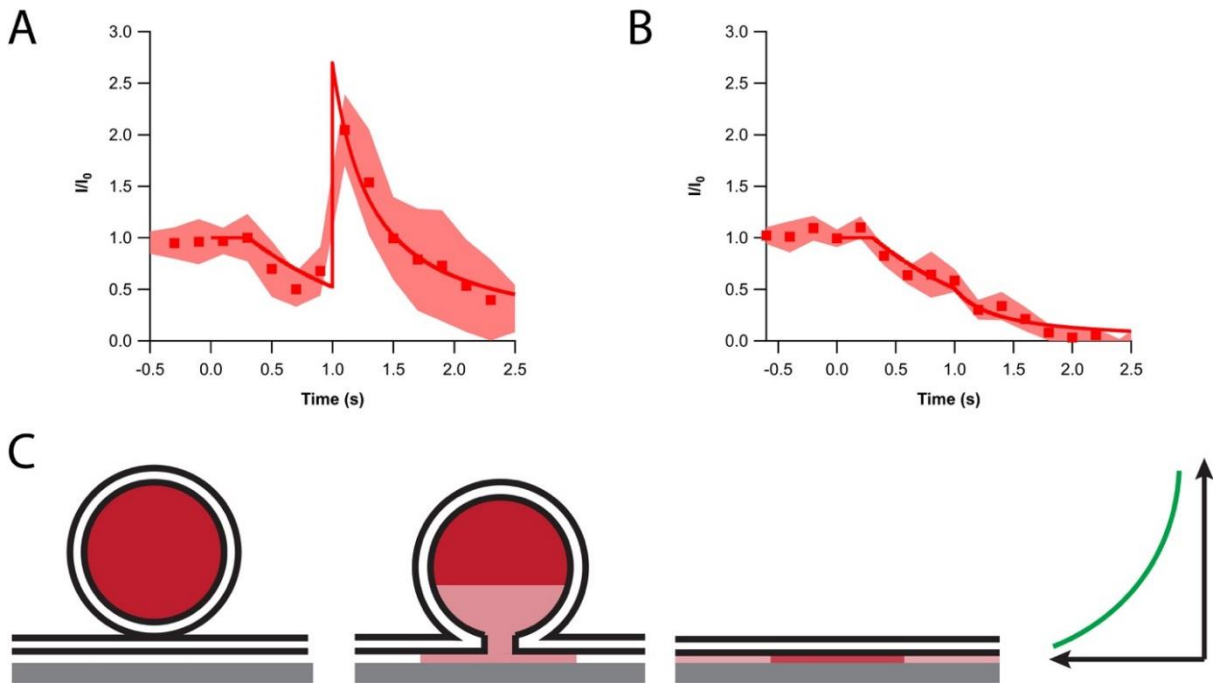

fig. S1. Line shape of intensity traces from single DCV fusion events. (**A**) Average peak pixel intensities (squares, with standard deviations shown as shades) from 10 individual DCV fusion events. The signals were aligned at the characteristic peak at t = 1s. DCV fusion was observed by TIRF microscopy as described in the Methods section. (**B**) Averaged peak pixel intensities (squares, with standard deviations shown as shades) from 5 individual DCV fusion events observed on an EPI fluorescence microscope. In this case, DCVs were docked under conditions of syntaxin-1a (1-288):SNAP-25 (lipid:protein of 3000) incubated with 0.5 µM Munc18 and 2 µM complexin-1. The undocked DCVs were washed out and fusion was trigged with Ca^{2+} and monitored using an EPI fluorescence microscope. (**C**) 2-step fusion/diffusion model to simulate the single DCV fluorescence data, which is described in detail in the Supplemental Text. The results of the simulations are shown in (A) and (B) as solid lines.

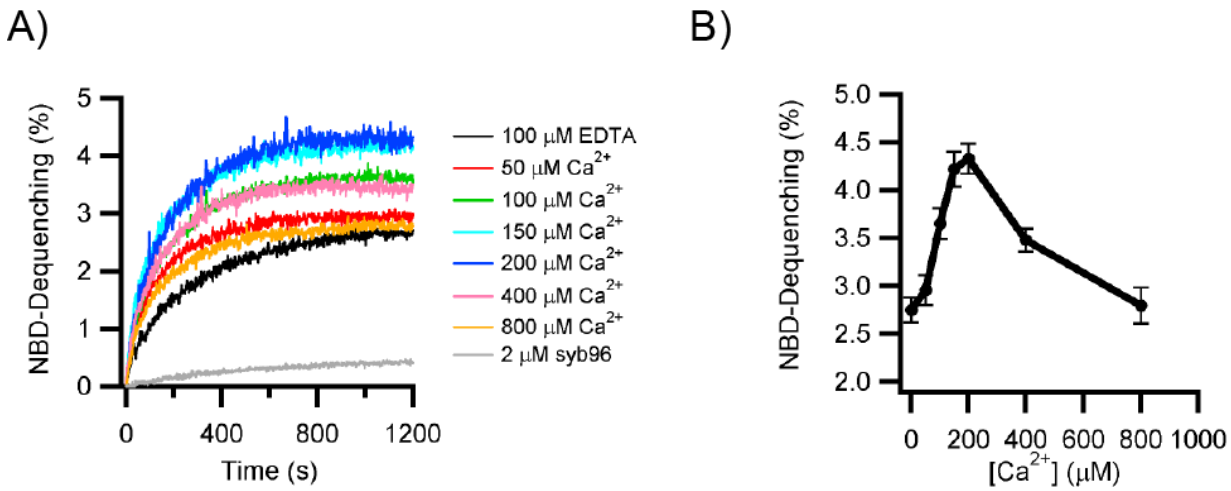

fig. S2. Ensemble lipid mixing of DCVs with reconstituted proteoliposomes containing syntaxin-1a (residues 183 to 288) (lipid/protein = 500) with a lipid composition of bPC:bPE:bPS:Chol:PI:PI(4,5)P_2:Rh-DOPE:NBD-DOPE (23.5:23.5:15:30:4:1:1.5:1.5) at increasing [Ca^{2+}]. (**A**) Shows averaged lipid mixing (4 traces) at increasing [Ca^{2+}] or in the presence of 2 μM inhibitor peptide syb(1-96). (**B**) Saturation of lipid mixing at increasing [Ca^{2+}]; error bars reflect standard error of repeated lipid mixing traces. Fitting the initial increase and saturation of the Ca^{2+} response results in a $K_{1/2}$ [Ca^{2+}] of 97 ± 18 μM. Summary of lipid mixing data is shown in table S4. The inhibition of lipid mixing at higher concentrations of calcium is due to charge screening of PI(4,5)P_2, as previously described (*19*).

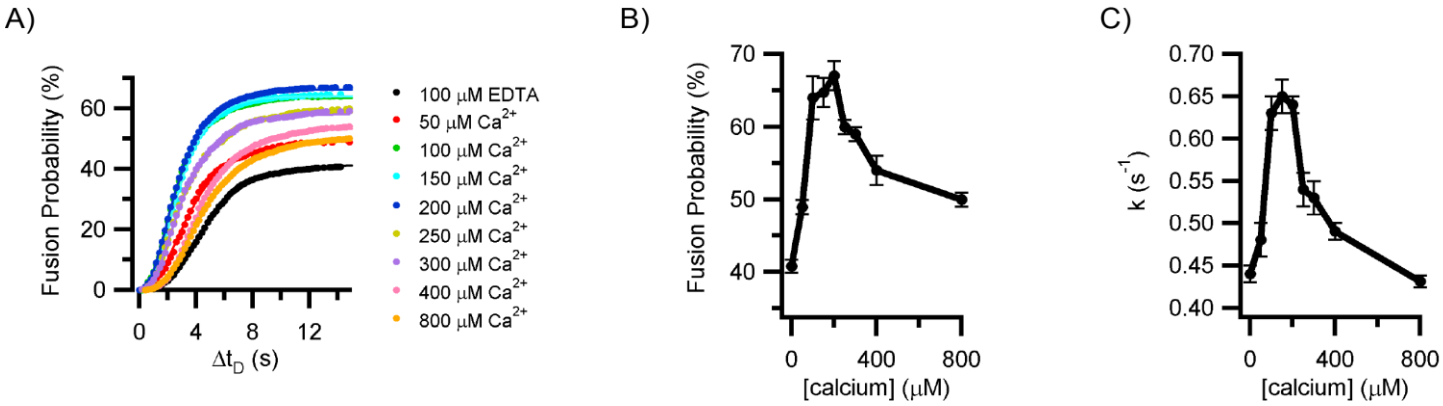

fig. S3. Single DCV fusion response. (**A**) Cumulative distribution function (normalized to fusion probability) of the delay time between docking and fusion (Δt_D) for single DCV fusion events fit with a parallel reaction model, $N(t) = N(1-e^{-kt})^m$ (*39*). (**B**) Fusion probability and (**C**) rate as a function of [Ca^{2+}]. Summary of docking and fusion and fit results are shown in tables S2 and S3, respectively. The inhibition of fusion at higher concentrations of calcium is due to charge screening of $PI(4,5)P_2$, as previously described (*19*).

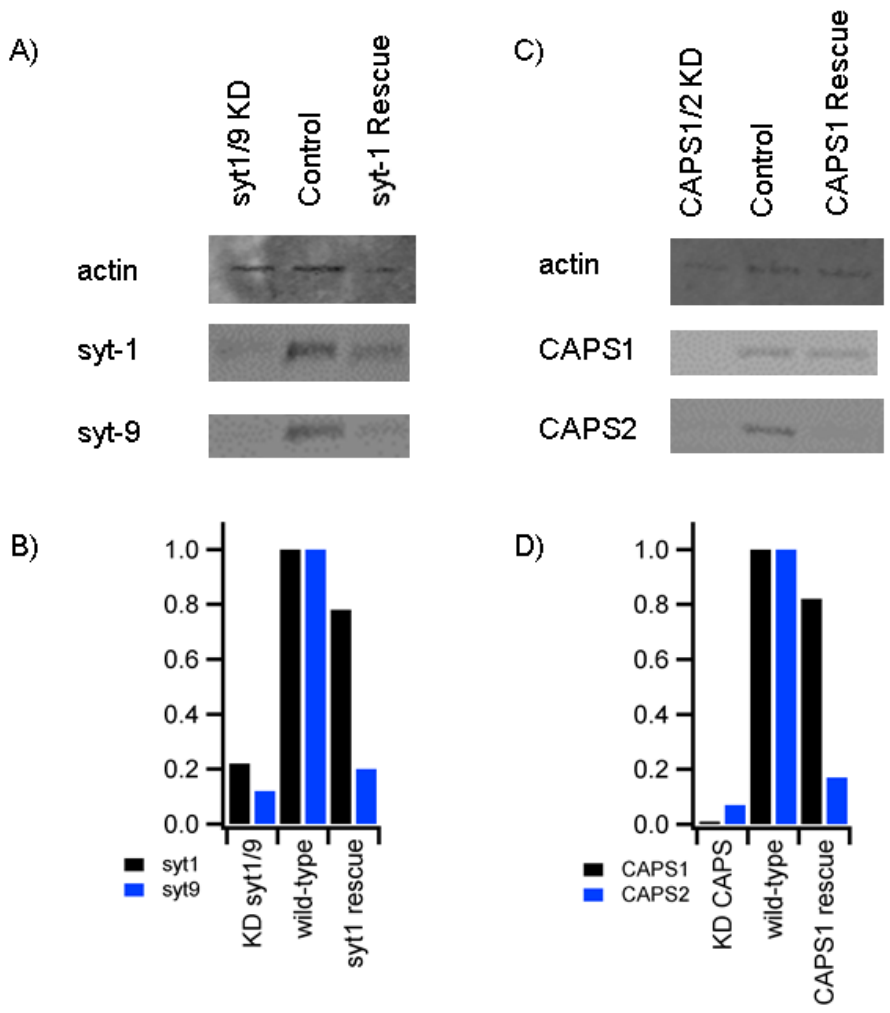

fig. S4. Quantification of shRNA-mediated knockdowns. Western blots of shRNA-mediated knockdowns for (**A**) syt1/9, which are the predominant isoforms of synaptotagmin in PC12 cells (*69*), or (**B**) CAPS1/2. Blots were of total cell lysates with approximately equal amounts of protein loaded onto each gel which was then normalized to total amount of actin per lysate to account for slight differences in total number of cells (B and **D**). (B) Syt1 was knocked down by ~80% while syt9 knockdown was ~85%. Rescue using a syt1 plasmid resulted in a recovery that was only 20% reduced from the wild-type. (D) CAPS1/2 knockdown depleted CAPS1 by ~95% and CAPS2 by ~90%. A CAPS1 plasmid resulted in a rescue that was about 20% reduced from wild-type CAPS1 levels.

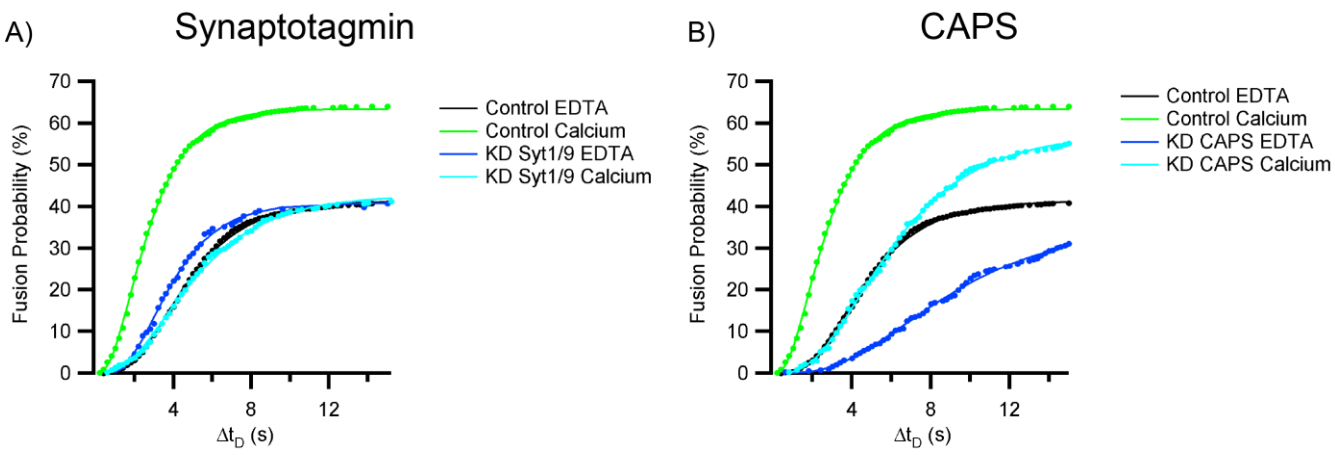

fig. S5. DCV fusion kinetics of synaptotagmin and CAPS knockdowns. Cumulative distribution functions of the delay time between docking and fusion of DCVs from knockdowns that deplete synaptotagmin (**A**) and CAPS (**B**). Summary of fitting results are shown in table S8.

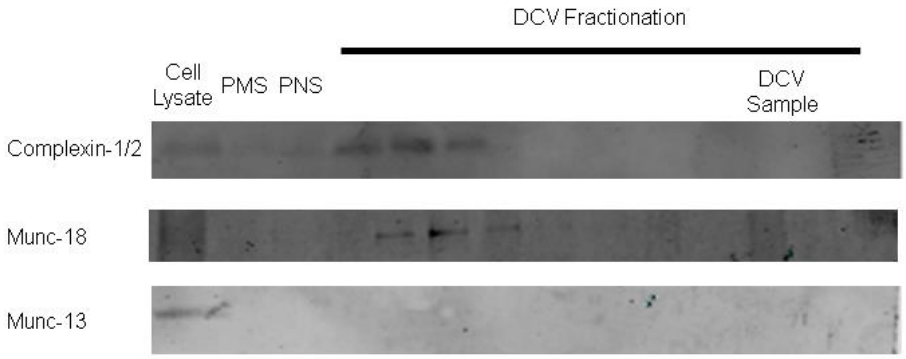

fig. S6. Western blots of complexin-1/2, Munc18, and Munc13 in fractions generated during DCV purification. DCV Sample identifies fraction 9 of the Optiprep gradient, which corresponds to fraction 9 in Fig. 1A. Both complexin 1/2 and Munc18 are detected in lower density gradient fractions but not in the DCV Sample. Munc13 also is not present in the DCV Sample and is detected only in the original cell lysate (left-most fraction). Most of Munc13 may have been pelleted with larger membranes during velocity sedimentation used to generate the PMS (postmitochondrial supernatant).

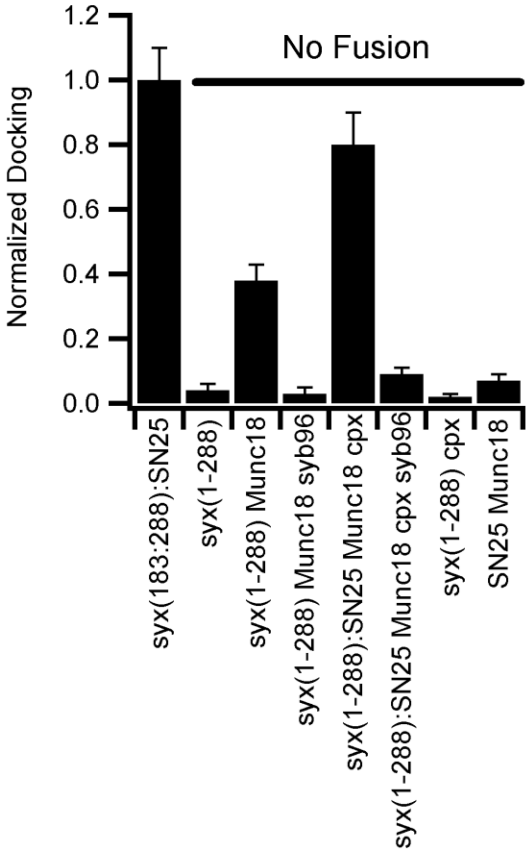

fig. S7. Controls to determine the effects of Munc18 and complexin-1 on docking to full-length syntaxin-1a (residues 1 to 288) and SNAP-25 and distinguish which of these conditions are inhibited by the soluble domain of synaptobrevin-2 (residues 1 to 96). Statistics are shown in table S17.

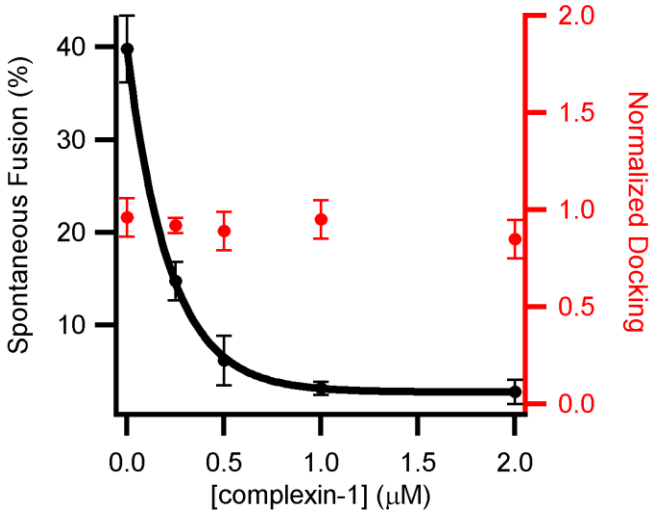

fig. S8. Complexin-1 inhibits fusion to planar supported bilayers containing syntaxin-1a (residues 1 to 288):SNAP-25 in the presence of 0.5 μM Munc18 in the absence of calcium, whereas there is no effect on DCV docking. Table S18 contains a summary of events.

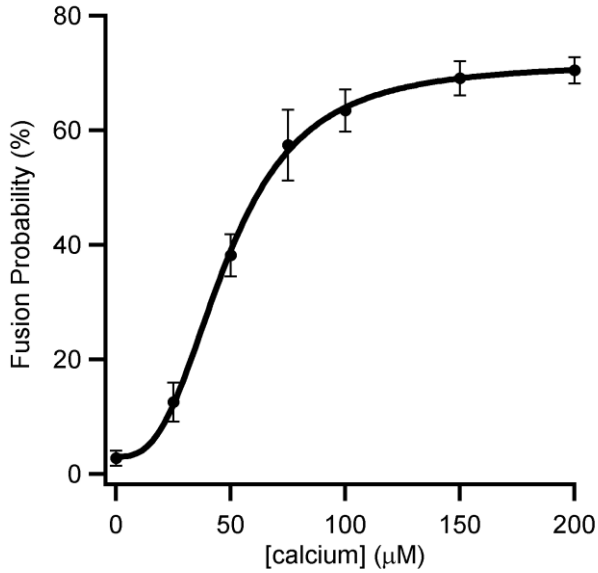

fig. S9. Fusion probability as a function of calcium for fusion of DCVs that were docked to planar supported bilayers with syntaxin-1a (residues 1 to 288):SNAP-25 in the presence of Munc18 and complexin-1 upon triggering with calcium. The cumulative distribution functions, from which these data were derived, are shown in Fig. 4B. The untriggered spontaneous fusion data point at 0 μM calcium is from Fig. 3D.

table S1. Event statistics for DCV docking and fusion to planar supported bilayers with syntaxin-1a (residues 183 to 288):SNAP-25 (lipid/protein = 3000), syntaxin-1a (residues 183 to 288) (lipid/protein = 3000), dodecylated SNAP-25 (lipid/protein = 3000), no protein, or syntaxin-1a (residues 183 to 288):SNAP-25 (lipid/protein = 3000) incubated with 2 µM synaptobevin-2 (residues 1 to 96) inhibitor peptide. All conditions were measured in the presence of 100 µM EDTA and 100 µM Ca^{2+}. Docking for all conditions was normalized to the docking observed with syntaxin-1a (183-288):SNAP-25 100 µM EDTA.

Condition	Number of Expiments	Normalized Docking	Percent Fusion	Total Number of Docking Events	Total Number of Fusion Events
syx(183-288):dSN25 EDTA	14	1.0 ± 0.1	41.0 ± 0.9	823	340
syx(183-288):dSN25 Ca^{2+}	7	3.0 ± 0.5	64.4 ± 3.0	1753	1184
syx(183-288) EDTA	5	0.14 ± 0.02	--	38	4
syx(183-288) Ca^{2+}	5	1.81 ± 0.09	--	468	7
dSN25 EDTA	5	0.15 ± 0.04	--	27	1
dSN25 Ca^{2+}	5	1.8 ± 0.3	--	351	6
Protein Free EDTA	5	0.19 ± 0.04	--	41	4
Protein Free Ca^{2+}	5	2.3 ± 0.2	--	434	7
syx(183-288):dSN25 syx(1-96) EDTA	5	0.10 ± 0.04	--	19	2
syx(183-288):dSN25 syx(1-96) Ca^{2+}	5	1.8 ± 0.1	--	368	3

table S2. Event statistics for DCV docking and fusion to planar supported bilayers with syntaxin-1a (residues 183 to 288):SNAP-25 (lipid/protein = 3000) with increasing concentration of divalent metals (Ca^{2+} and Mg^{2+}). Docking for all conditions was normalized to the docking observed in 100 μM EDTA.

Condition	Number of Experiments	Normalized Docking	Percent Fusion	Total Number of Docking Events	Total Number of Fusion Events
100 μM EDTA	14	1.0 ± 0.1	40.1 ± 0.9	823	340
50 μM Ca^{2+}	5	2.2 ± 0.4	49 ± 1	817	394
100 μM Ca^{2+}	7	3.0 ± 0.5	64 ± 3	1753	1184
150 μM Ca^{2+}	5	4.1 ± 0.4	64.7 ± 0.5	1840	1188
200 μM Ca^{2+}	5	7.5 ± 0.8	67 ± 1	3233	2169
250 μM Ca^{2+}	5	7.7 ± 0.3	60 ± 1	1150	693
300 μM Ca^{2+}	5	9.0 ± 0.6	59 ± 1	1343	797
400 μM Ca^{2+}	5	10.8 ± 1.1	54 ± 2	3264	1766
800 μM Ca^{2+}	5	11.6 ± 1.4	50 ± 1	3965	1968
100 μM Mg^{2+}	5	1.7 ± 0.2	45 ± 2	320	145
1000 μM Mg^{2+}	5	1.8 ± 0.3	50 ± 2	306	155

table S3. Fit values of a parallel reaction model [$N(t) = N(1 - e^{-kt})^m$, where N is the fusion probability, k is the rate, and m is the number of parallel reactions occurring] for the cumulative distribution function of delay times between docking and fusion for single-particle DCV events with different concentrations of divalent metals. Experimental traces are shown in Fig. 1F and fig. S4. Planar bilayers contained syntaxin-1a (183-288):SNAP-25 (lipid:protein 3000) and lipid composition 25:25:15:30:4:1 bPC:bPE: bPS:Chol:PI:PI4,5P_2).

Condition	Number of Experiments	k (s^{-1})	m
100 µM EDTA	14	0.44 ± 0.01	4.8 ± 0.2
50 µM Ca^{2+}	5	0.48 ± 0.02	3.3 ± 0.2
100 µM Ca^{2+}	7	0.63 ± 0.02	3.1 ± 0.1
150 µM Ca^{2+}	5	0.65 ± 0.02	3.7 ± 0.1
200 µM Ca^{2+}	5	0.61 ± 0.01	3.0 ± 0.1
250 µM Ca^{2+}	5	0.54 ± 0.02	3.0 ± 0.1
300 µM Ca^{2+}	5	0.53 ± 0.02	3.2 ± 0.1
400 µM Ca^{2+}	5	0.49 ± 0.01	5.3 ± 0.2
800 µM Ca^{2+}	5	0.43 ± 0.01	4.4 ± 0.1
100 µM Mg^{2+}	5	0.39 ± 0.04	3.4 ± 0.4
1000 µM Mg^{2+}	5	0.35 ± 0.03	2.6 ± 0.2

table S4. Fits of ensemble lipid mixing data shown in fig. S3. Averages of 4 traces were taken for each condition. All curves with fit with a two-component model being $y = A_1(1\text{-}e^{-k1*t})+A_2(1\text{-}e^{-k2*t})$.

[Ca^{2+}]	Saturation	k_1 (s^{-1})	k_2 (s^{-1})
0	2.8 ± 0.1	0.0028 ± 0.0001	0.022 ± 0.003
50	3.0 ± 0.2	0.0048 ± 0.0001	0.024 ± 0.003
100	3.7 ± 0.2	0.0044 ± 0.0001	0.03 ± 0.003
150	4.2 ± 0.2	0.0041 ± 0.0001	0.026 ± 0.002
200	4.3 ± 0.2	0.0047 ± 0.0001	0.037 ± 0.007
400	3.5 ± 0.1	0.0056 ± 0.0001	0.07 ± 0.01
800	2.8 ± 0.2	0.0040 ± 0.0001	0.025 ± 0.002

table S5. Event statistics for docking and fusion of DCVs to planar supported bilayers with 5% PI(4,5)P_2 [bPC:bPE:bPS:Chol:PI(4,5)P_2 (25:25:15:30:5)], 3% PI(4,5)P_2 [bPC:bPE:bPS:Chol:PI:PI(4,5)P_2 (25:25:15:30:2:3)], 1% PI(4,5)P_2 [bPC:bPE:bPS:Chol:PI:PI(4,5)P_2 (25:25:15:30:4:1)], 0% PI(4,5)P_2 [bPC:bPE:bPS:Chol:PI (25:25:15:30:5)], and no charged lipids [bPC:bPE:Chol (35:35:30)] in the presence of 100 µM EDTA or 100 µM Ca^{2+}. Graphs of data are shown in Fig. 1H. Docking for all conditions was normalized to the docking observed with 1% PI4,5P_2 in the presence of EDTA.

Condition	Number of Experiments	Normalized Docking	Percent Fusion	Total Number of Docking Events	Total Number of Fusion Events
5% PI4,5P_2 - EDTA	5	1.2 ± 0.1	36 ± 1	294	108
5% PI4,5P_2 Ca^{2+}	5	4.8 ± 0.6	76 ± 2	1223	932
3% PI4,5P_2 - EDTA	5	1.1 ± 0.1	42 ± 1	280	120
3% PI4,5P_2 Ca^{2+}	4	4.0 ± 0.2	75 ± 2	822	611
1% PI4,5P_2 - EDTA	14	1.0 ± 0.1	41 ± 1	823	340
1% PI4,5P_2 Ca^{2+}	7	3.0 ± 0.5	64 ± 3	1753	1184
0% PI4,5P_2 - EDTA	5	0.9 ± 0.1	38 ± 3	211	82
0% PI4,5P_2 Ca^{2+}	6	1.3 ± 0.1	47 ± 3	386	183
No Charge - EDTA	5	1.2 ± 0.2	47 ± 2	274	133
No Charge – Ca^{2+}	5	1.1 ± 0.1	45 ± 4	259	117

table S6. Event statistics for docking and fusion of DCVs to planar supported bilayers with 5% $PI(4,5)P_2$ [bPC:bPE:bPS:Chol:$PI(4,5)P_2$ (25:25:15:30:5)], 3% $PI(4,5)P_2$ [bPC:bPE:bPS:Chol:PI:$PI(4,5)P_2$ (25:25:15:30:2:3)], 1% $PI(4,5)P_2$ [bPC:bPE:bPS:Chol:PI:$PI(4,5)P_2$ (25:25:15:30:4:1)], 0% $PI(4,5)P_2$ [bPC:bPE:bPS:Chol:PI (25:25:15:30:5)], and no charged lipids [bPC:bPE:Chol (35:35:30)] in the presence of 100 µM EDTA or 100 µM Ca^{2+}. Graphs of data are shown in Fig. 1H. The fit is of a parallel reaction model being $N(t) = N(1-e^{-kt})^m$ where N is the fusion probability, k is the rate, and m is the number of parallel reactions occurring.

Condition	k (s^{-1})	m
5% $PI4,5P_2$ - EDTA	0.35 ± 0.05	3.5 ± 0.5
5% $PI4,5P_2$ - Ca^{2+}	0.63 ± 0.05	2.4 ± 0.2
3% $PI4,5P_2$ - EDTA	0.36 ± 0.04	2.8 ± 0.3
3% $PI4,5P_2$ - Ca^{2+}	0.61 ± 0.05	2.4 ± 0.1
1% $PI4,5P_2$ - EDTA	0.44 ± 0.10	4.8 ± 0.2
1% $PI4,5P_2$ - Ca^{2+}	0.63 ± 0.02	3.1 ± 0.1
0% $PI4,5P_2$ - EDTA	0.42 ± 0.05	4.9 ± 0.8
0% $PI4,5P_2$ - Ca^{2+}	0.35 ± 0.03	3.3 ± 0.3
No Charge - EDTA	0.42 ± 0.03	4.4 ± 0.5
No Charge – Ca^{2+}	0.43 ± 0.04	4.0 ± 0.5

table S7. Event statistics for DCV docking and fusion to planar supported bilayers with syntaxin-1a (residues 183 to 288):SNAP-25 (lipid/protein = 3000) with wild-type DCVs, DCVs inhibited with antibodies for either syt or CAPS, or DCVs that have had syt or CAPS knocked down using shRNA before purification. Graphs of data are shown in Fig. 2. Docking for all conditions was normalized to the docking observed in the wild-type EDTA sample.

Condition	Number of Experiments	Normalized Docking	Percent Fusion	Total Number of Docking Events	Total Number of Fusion Events
Wild-type EDTA	14	1.0 ± 0.1	41.0 ± 0.9	823	340
Wild-type Ca^{2+}	7	3.0 ± 0.5	64 ± 3	1753	1184
Anti-syt1/9 EDTA	5	1.2 ± 0.2	45 ± 1	244	108
Anti-syt1/9 Ca^{2+}	5	2.9 ± 0.3	42 ± 1	769	335
KD syt1/9 EDTA	5	1.00 ± 0.03	41 ± 3	234	98
KD syt1/9 Ca^{2+}	5	2.8 ± 0.2	41 ± 3	574	236
syt1 rescue EDTA	5	1.0 ± 0.2	41 ± 3	225	93
syt1 rescue Ca^{2+}	5	2.6 ± 0.2	66 ± 2	585	384
Anti-CAPS1/2 EDTA	5	1.0 ± 0.1	44 ± 3	214	95
Anti-CAPS1/2 Ca^{2+}	5	1.0 ± 0.1	65 ± 3	311	202
CAPS KD EDTA	5	1.0 ± 0.2	31 ± 3	410	127
CAPS KD Ca^{2+}	5	1.2 ± 0.2	55 ± 2	504	278
CAPS rescue EDTA	5	1.0 ± 0.1	46 ± 3	259	118
CAPS rescue Ca^{2+}	5	2.9 ± 0.4	66 ± 3	741	495

table S8. Fit values of a parallel reaction model [$N(t) = N(1 - e^{-kt})^m$, where N is the fusion probability, k is the rate, and m is the number of parallel reactions occurring] for the cumulative distribution function of delay times between docking and fusion for single-particle DCV events for conditions described in Fig. 2. DCVs were inhibited using antibodies for synaptotagmin or CAPS or prepared from syt- or CAPS-deficient cell lines generated by RNAi.

Condition	Number of Experiments	k (s^{-1})	m
Control EDTA	14	0.40 ± 0.10	4.8 ± 0.2
Control Ca^{2+}	7	0.63 ± 0.02	3.1 ± 0.1
Anti-syt1/9 EDTA	5	0.45 ± 0.04	6.0 ± 1.0
Anti-syt1/9 Ca^{2+}	5	0.47 ± 0.02	6.0 ± 0.5
KD syt1/9 EDTA	5	0.54 ± 0.06	5.1 ± 0.8
KD syt1/9 Ca^{2+}	5	0.35 ± 0.02	3.5 ± 0.3
syt1 rescue EDTA	5	0.31 ± 0.04	2.6 ± 0.3
syt1 rescue Ca^{2+}	5	0.45 ± 0.02	2.1 ± 0.1
Anti-CAPS1/2 EDTA	5	0.44 ± 0.05	3.9 ± 0.6
Anti-CAPS1/2 Ca^{2+}	5	0.54 ± 0.04	2.9 ± 0.3
CAPS KD EDTA	5	0.23 ± 0.02	4.2 ± 0.5
CAPS KD Ca^{2+}	5	0.31 ± 0.02	3.7 ± 0.3
CAPS rescue EDTA	5	0.40 ± 0.04	3.8 ± 0.5
CAPS rescue Ca^{2+}	5	0.53 ± 0.03	2.2 ± 0.2

table S9. Event statistics for DCV docking and fusion to planar supported bilayers containing either syntaxin-1a (residues 183 to 288) or syntaxin-1a (residues 1 to 288) with SNAP-25 (lipid/protein = 3000), with the addition of complexin-1 and/or Munc18 in the presence of 100 µM EDTA or 100 µM Ca^{2+}. Graphs of data is shown in Fig. 3. Docking for all conditions was normalized to the docking observed for the syntaxin-1a (183-288):SNAP25 in EDTA sample.

	Condition	Number of Experiments	Normalized Docking	Percent Fusion	Total Number of Docking Events	Total Number of Fusion Events
syntaxin-1a(183-288): d-SNAP-25	EDTA	14	1.0 ± 0.1	40.1 ± 0.9	823	340
	Ca^{2+}	7	3.0 ± 0.5	64 ± 3	1753	1184
	Munc18 EDTA	5	1.0 ± 0.1	44 ± 2	376	167
	Munc18 Ca2+	5	3.0 ± 0.2	67 ± 2	957	651
	complexin-1 EDTA	5	0.19 ± 0.05	N/A	38	2
	complexin-1 Ca2+	5	2.9 ± 0.3	64 ± 1	779	497
	Munc18 complexin-1 EDTA	5	0.1 ± 0.1	N/A	39	8
	Munc18 complexin-1 Ca2+	5	2.4 ± 0.2	62 ± 2	680	422
syntaxin-1a(1-288): d-SNAP-25	EDTA	5	0.3 ± 0.1	30 ± 2	160	49
	Ca^{2+}	5	3.3 ± 0.3	45 ± 2	766	342
	Munc18 EDTA	5	1.0 ± 0.1	40 ± 4	333	142
	Munc18 Ca2+	5	3.2 ± 0.2	56 ± 2	473	268
	complexin-1 EDTA	5	0.08 ± 0.02	N/A	22	1
	complexin-1 Ca2+	5	2.8 ± 0.4	16 ± 3	718	119
	Munc18 complexin-1 EDTA	5	0.8 ± 0.1	2 ± 1	203	6
	Munc18 complexin-1 Ca2+	5	3.0 ± 0.1	60 ± 2	456	274

table S10. Fit values of a parallel reaction model [$N(t) = N(1 - e^{-kt})^m$, where N is the fusion probability, k is the rate, and m is the number of parallel reactions occurring] for the cumulative distribution function of delay times between docking and fusion for single-particle DCV events for conditions described in Fig. 3.

	Condition	Number of Experiments	k (s^{-1})	m
syntaxin-1a(183-288): d-SNAP-25	EDTA	14	0.43 ± 0.01	4.4 ± 0.2
	Ca^{2+}	7	0.63 ± 0.02	3.1 ±0.1
	Munc18 EDTA	5	0.38 ± 0.03	2.3 ± 0.2
	Munc18 Ca^{2+}	5	0.56 ± 0.02	2.5 ± 0.1
	complexin-1 EDTA	5	--	--
	complexin-1 Ca^{2+}	5	0.57 ± 0.02	3.5 ± 0.2
	Munc18 complexin-1 EDTA	5	--	--
	Munc18 complexin-1 Ca^{2+}	5	0.58 ± 0.02	2.7 ± 0.1
syntaxin-1a(1-288): d-SNAP-25	EDTA	5	0.37 ± 0.07	4.0 ± 0.9
	Ca^{2+}	5	0.43 ± 0.02	2.7 ± 0.2
	Munc18 EDTA	5	0.51 ± 0.04	3.9 ± 0.4
	Munc18 Ca^{2+}	5	0.56 ± 0.03	3.9 ± 0.3
	complexin-1 EDTA	5	--	--
	complexin-1 Ca^{2+}	5	0.36 ± 0.04	2.6 ± 0.3
	Munc18 complexin-1 EDTA	5	--	--
	Munc18 complexin-1 Ca^{2+}	5	0.59 ± 0.03	3.8 ± 0.3

table S11. Event statistics of triggered fusion of DCVs at different calcium concentrations from data shown in Fig. 4B. The data are well described by a first order kinetic fit, $N(t) = N(1-e^{-kt})$.

Condition	Number of Experiments	Fusion Probability	Docked Events	Triggered Fusion	k (s^{-1})
25 µM Ca^{2+}	5	12 ± 3	541	61	0.06 ± 0.01
50 µM Ca^{2+}	5	38 ± 4	279	101	0.06 ± 0.01
75 µM Ca^{2+}	5	57 ± 6	913	534	0.110 ± 0.006
100 µM Ca^{2+}	5	63 ± 4	723	462	0.190 ± 0.007
150 µM Ca^{2+}	5	69 ± 3	425	291	0.194 ± 0.008
200 µM Ca^{2+}	5	70 ± 2	903	629	0.185 ± 0.006

table S12. Event statistics of spontaneous fusion of DCVs docked in triggering conditions with planar supported bilayers of different lipid compositions. Data are shown in Fig. 4D. Docking has been normalized to the docking observed in the No Charge sample.

Condition	Number of Experiments	Normalized Docking	Percent Fusion	Total Number of Docking Events	Total Number of Fusion Events
5% PI4,5P_2	5	1.1 ± 0.1	1.4 ± 0.6	307	5
3% PI4,5P_2	5	1.0 ± 0.1	2.3 ± 0.8	264	6
1% PI4,5P_2	5	0.8 ± 0.1	3 ± 1	203	6
0% PI4,5P_2	5	0.8 ± 0.1	3 ± 1	208	7
No Charge	5	1.0 ± 0.1	8 ± 3	247	23

table S13. Event statistics of triggered fusion of DCVs with planar supported bilayers of different lipid compositions. All events were triggered with 100 µM Ca^{2+}. Data are shown in Fig. 4D. The data are well described by a first order kinetic fit, $N(t) = N(1-e^{-kt})$.

Condition	Number of Experiments	Percent Fusion	Total Number of Docking Events	Total Number of Fusion Events	k (s^{-1})	m
5% PI4,5P_2	4	77 ± 1	196	151	0.26 ± 0.04	0.8 ± 0.05
3% PI4,5P_2	5	71 ± 2	381	270	0.26 ± 0.02	1.0 ± 0.1
1% PI4,5P_2	5	63 ± 2	723	462	0.23 ± 0.02	1.1 ± 0.1
0% PI4,5P_2	4	33 ± 2	568	185	0.16 ± 0.01	1.9 ± 0.1
No Charge	5	12 ± 2	804	103	0.17 ± 0.03	2.8 ± 0.4

table S14. Event statistics of spontaneous fusion of DCVs docked in triggering conditions with knockdowns of syt-1/9 or CAPS with subsequent recoveries. Data are shown in Fig. 4E.

Condition	Number of Experiments	Normalized Docking	Percent Fusion	Total Number of Docking Events	Total Number of Fusion Events
Wild-type	5	0.8 ± 0.1	3 ± 1	206	6
syt1/9 KD	5	0.9 ± 0.1	3 ± 1	227	8
syt1 rescue	5	0.8 ± 0.1	3 ± 1	335	12
CAPS KD	5	0.8 ± 0.1	4 ± 2	345	12
CAPS1 rescue	5	0.9 ± 0.1	4 ± 1	226	10
CAPS KD – C1C2Mun rescue	5	0.9 ± 0.1	3 ± 1	356	11

table S15. Event statistics of triggered fusion of DCVs with knockdowns of syt-1/9 or CAPS and subsequent recoveries. All events were triggered with 100 µM Ca^{2+}. Data are shown in Fig. 4E. The data are well described by a first order kinetic fit, $N(t) = N(1-e^{-kt})$.

Condition	Number of Experiments	Fusion Probability	Docked Events	Triggered Fusion	k (s^{-1})
Wild-type	5	64 ± 4	723	462	0.190 ± 0.007
syt1/9 KD	5	6 ± 2	314	21	--
syt1 rescue	5	63 ± 2	227	145	0.189 ± 0.005
CAPS KD	5	20 ± 3	701	147	0.09 ± 0.03
CAPS1 rescue	5	65 ± 2	281	183	0.19 ± 0.01
CAPS KD – C1C2Mun rescue	5	70 ± 2	524	375	0.195 ± 0.008

table S16. Table of primers described in the "Plasmids and shRNA constructs" section of Materials and Methods. Mismatches/mutations are highlighted in bold and restriction sites are underlined.

#	Name	Sequence (5'->3')
1	ins_BstZ17I_fw	AGATCTTGAGACAAATGGCAGTATACATCCACAATTTTAAAAG
2	ins_EcoRI_rv	TGCCATTTGTCTCAAGATCTAGAATTCTCCCCTCGGGGTTG
3	TRC1.5_shRNA_MfeI_fw	TATTCAATTGTTCACCGAGGGCCTATTTC
4	TRC2_shRNA_MfeI_fw	TATTCAATTGGGCCTATTTCCCATGATTCC
5	TRC_shRNA_BstZ17I_rv	AGCTAAGTATACGGATGAATACTGCCATTTGTC
6	CAPS1_shRNA	TTGTGGAAAGGACGAGGTACCGGTCGTCTTCTTCATCTTCCTCGTCACT GTGAAGCTTGATAGTGATGAGGAGGATGAGGAAGACGACTATTTTTTG AATTCTAGATCTTGAGACAAATGG
7	syt1_del_pHluorin_fw	CTACTCTTGTGCCAGGGTGTGGTCTCCTCAGGCGGAAGCGGAGGC
8	syt1_del_pHluorin_rv	CTTCTTGACAGCCAGCATGGCATC
9	syt1_shRNA-resist_fw	TCGA**A**CA**G**AT**T**CAGAA**G**GTGCA**G**GTGGTGGTAACTG
10	syt1_shRNA-resist_rv	ACCAC**C**TGCAC**C**TTCTG**A**AT**C**TG**T**TCGAACGGAACTTC

table S17. Event statistics for DCV docking and fusion to planar supported bilayers with the indicated combination of proteins syntaxin-1a (residues 183 to 288), syntaxin-1a (residues 1 to 288), and SNAP-25 (lipid/protein = 3000) incubated, as indicated, with Munc18 (0.5 μM), complexin-1 (2 μM), and synaptobrevin-2 (residues 1 to 96) inhibitor peptide. All conditions were measured in the presence of 100 μM EDTA. Docking has been normalized to the docking observed in the syx(183-288):dSN25 sample.

Condition	Number of Experiments	Normalized Docking	Percent Fusion	Total Number of Docking Events	Total Number of Fusion Events
syx(183-288):dSN25	14	1.0 ± 0.1	41.0	823	340
syx(1-288)	5	0.04 ± 0.02	--	17	1
syx(1-288), Munc18	5	0.38 ± 0.5	--	173	4
syx(1-288), Munc18, syb96	5	0.03 ± 0.02	--	15	1
syx(1-288):dSN25, Munc18, cpx	5	0.8 ± 0.1	--	203	6
syx(1-288):dSN25, Munc18, cpx, syb96	5	0.09 ± 0.02	--	41	1
syx(1-288), cpx	5	0.01 ± 0.01	--	5	0
dSN25, Munc18	5	0.07 ± 0.02	--	31	1

table S18. Event statistics for DCV docking and fusion to planar supported bilayers containing syntaxin-1a (residues 1 to 288):SNAP-25, 0.5 μM Munc18, and indicated amounts of complexin-1. Docking has been normalized to that observed in the 0 μM cpx sample.

Condition	Number of Experiments	Normalized Docking	Percent Fusion	Total Number of Docking Events	Total Number of Fusion Events
0 μM cpx	5	1.0 ± 0.1	40 ± 5	313	142
0.25 μM cpx	4	0.92 ± 0.04	15 ± 2	147	22
0.5 μM cpx	5	0.9 ± 0.0.1	6 ± 3	235	15
1 μM cpx	5	1.0 ± 0.1	3 ± 1	252	8
2 μM cpx	5	0.8 ± 0.1	3 ± 1	203	6